J|A|C|S
ARTICLES
Published on Web 05/23/2002

Dynamic Docking and Electron Transfer between Zn-myoglobin and Cytochrome b_5

Zhao-Xun Liang,† Judith M. Nocek,† Kai Huang,† Ryan T. Hayes,† Igor V. Kurnikov,† David N. Beratan,‡ and Brian M. Hoffman*,†

Contribution from the Department of Chemistry, Northwestern University, 2145 Sheridan Road, Evanston, Illinois 60208, and Department of Chemistry, Duke University, Durham, North Carolina 27708

Received December 13, 2001

Abstract: We present a broad study of the effect of neutralizing the two negative charges of the Mb propionates on the interaction and electron transfer (ET) between horse Mb and bovine cyt b_5, through use of Zn-substituted Mb (ZnMb, **1**) to study the photoinitiated reaction, $(^3ZnP)Mb + Fe^{3+}$cyt $b_5 \rightarrow (ZnP)^+Mb + Fe^{2+}$cyt b_5. The charge neutralization has been carried out both by replacing the Mb heme with zinc-deuteroporphyrin dimethylester (ZnMb(dme), **2**), which replaces the charges by small neutral hydrophobic patches, and also by replacement with the newly prepared zinc-deuteroporphyrin diamide (ZnMb(diamide), **3**), which converts the charged groups to neutral, hydrophilic ones. The effect of propionate neutralization on the conformation of the zinc-porphyrin in the Mb heme pocket has been studied by multinuclear NMR with an ^{15}N labeled zinc porphyrin derivative (ZnMb(^{15}N-diamide), **4**). The rates of photoinitiated ET between the Mb's (**1**−**3**) and cyt b_5 have been measured over a range of pH values and ionic strengths. Isothermal titration calorimetry (ITC) and NMR methods have been used to independently investigate the effect of charge neutralization on Mb/b_5 binding. The neutralization of the two heme propionates of ZnMb by formation of the heme diester or, for the first time, the diamide increases the second-order rate constant of the ET reaction between ZnMb and cyt b_5 by as much as several 100-fold, depending on pH and ionic strength, while causing negligible changes in binding affinity. Brownian dynamic (BD) simulations and ET pathway calculations provide insight into the protein docking and ET process. The results support a new "dynamic docking" paradigm for protein−protein reactions in which numerous weakly bound conformations of the docked complex contribute to the binding of cyt b_5 to Mb and Hb, but only a very small subset of these are ET active, and this subset does not include the conformations most favorable for binding; the Mb surface is a large "target" with a small "bullseye" for the cyt b_5 "arrow". This paradigm differs sharply from the more familiar, "simple" docking within a single, or narrow range of conformations, where binding strength and ET reactivity increase in parallel. Likewise, it is distinct from, although complementary to, the well-known picture of conformational control of ET through "gating", or a related picture of "conformational coupling". The new model describes situations in which tight binding does not correlate with efficient ET reactivity, and explains how it is possible to modulate reactivity without changing affinity. Such "decoupling" of reactivity from binding clearly is of physiological relevance for the reduction of met-Mb in muscle and of met-Hb in a red cell, where tight binding of cyt b_5 to the high concentration of ferrous-Mb/Hb would prevent the cytochrome from finding and reducing the oxidized proteins; it likely is of physiological relevance in other situations, as well.

Introduction

Cytochrome b_5 (cyt b_5) is a small heme protein (11 kDa) which performs a physiological repair function in erythrocytes, where it reduces met-hemoglobin (Hb) back to the oxygen-binding ferrous form.[1−3] A similar reductase system involving cyt b_5 has also been suggested to exist in muscle, where it functions to reduce met-myoglobin back to deoxy-myoglobin.[4−6] In early studies of the interaction between Mb and cyt b_5, Mauk and co-workers[7] did not detect an obvious UV−vis difference spectrum caused by interactions between horse heart Mb and bovine liver cyt b_5, indicating that these two form at most a weak protein−protein complex. In contrast, La Mar and co-workers reported that bovine heart Fe^{3+}Mb and bovine liver cyt b_5 form a 1:1 electrostatic complex at low pH (5.6) with a

* To whom correspondence should be addressed. E-mail: bmh@nwu.edu.
† Northwestern University.
‡ Duke University.

(1) Abe, K.; Sugita, Y. *Eur. J. Biochem.* **1979**, *101*, 423−428.
(2) Mauk, M. R.; Mauk, A. G. *Biochemistry* **1982**, *21*, 4730−4734.
(3) Bunn, H. F.; Forget, B. G. *Hemoglobin: Molecular, Genetic, and Clinical Aspects*; W. B. Saunders Co.: Philadelphia, 1986.
(4) Hagler, L.; Coppes, R. I., Jr.; Herman, R. H. *J. Biol. Chem.* **1979**, *254*, 6505−6514.
(5) Livingston, D. J.; McLachlan, S. J.; La Mar, G. N.; Brown, W. D. *J. Biol. Chem.* **1985**, *260*, 15699−15707.
(6) Arihara, K.; Cassens, R. G.; Greaser, M. L.; Luchansky, J. B.; Mozdziak, P. E. *Meat Sci.* **1995**, *39*, 205−213.
(7) Mauk, M. R.; Reid, L. S.; Mauk, A. G. *Biochemistry* **1982**, *21*, 1843.

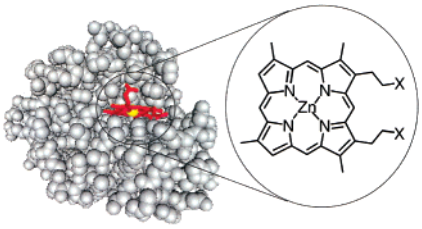

Figure 1. Schematic view of Zn-deuteroporphyrin-substituted Mb's (ZnMb's).

much larger association constant, $K_a > 10^5$ M.[5] Recently, we confirmed that the binding affinity of horse Mb for bovine cyt b_5 is very low, even under low ionic strength conditions, and that the weak interaction between Mb and cyt b_5 is dominated by electrostatic interactions;[8] analogous results hold for Hb.[9,10] While cyt b_5 has a distinct negatively charged patch as the putative binding domain for protein docking, Brownian dynamics (BD) simulation and NMR studies have suggested that a broad region encompassing almost the entire hemisphere surrounding the exposed Mb heme edge may act as the docking interface of the Mb/cyt b_5 interaction.[8,11]

Surface electrostatic potential analysis of Mb shows a positively charged region around the exposed heme edge, within which the two heme propionates present a pair of negative charges that tend to repel the negatively charged cyt b_5.[8,12,13] Simple electrostatic considerations thus suggest that the neutralization of these two negative charges would enhance the affinity of Mb for cyt b_5. However, in a preliminary study, we found that the neutralization of two negative charges by methylation of the propionates increased the overall rate of photoinitiated, $(^3ZnP)Mb + Fe^{3+}cyt\ b_5 \rightarrow (ZnP)^+Mb + Fe^{2+}cyt\ b_5$, ET by about 100-fold without significantly enhancing myoglobin's affinity for cyt b_5.[14] To interpret this finding, we suggested that cyt b_5 can dock within a broad region of the Mb surface, but that only a small fraction of the docking surface is ET reactive.

Herein, we present a broad study of the effects of neutralizing the two negative charges of the Mb propionates, Figure 1, on the interaction and ET between zinc-substituted horse Mb (ZnMb, **1**) and bovine cyt b_5. The charge neutralization has been carried out both by replacing the Mb heme with zinc-deuteroporphyrin dimethylester (ZnMb(dme), **2**), which replaces the charges by small neutral hydrophobic patches, and also by replacement with the newly prepared zinc-deuteroporphyrin diamide (ZnMb(diamide), **3**), which converts the charged groups to neutral, hydrophilic ones. The effect of propionate neutralization on the conformation of zinc-porphyrin in the Mb heme pocket has been studied by multinuclear NMR with an ^{15}N labeled zinc porphyrin derivative (ZnMb(^{15}N-diamide), **4**). The rates of photoinitiated ET between the Mb's (**1**−**3**) and cyt b_5 have been measured with these over a range of pH values and ionic strengths. Isothermal titration calorimetry (ITC) and NMR methods have been used to independently investigate the effect of charge neutralization on Mb/b_5 binding. Brownian dynamic (BD) simulations and ET pathway calculations provide insight into the protein docking and ET process.

The results support a new "dynamic docking" paradigm for protein−protein reactions in which numerous weakly bound conformations of the docked complex contribute to the binding of cyt b_5 to Mb and Hb. Only a very small subset of these are ET active, and the most reactive conformations are not the most favorable for binding. The new model describes situations in which binding is in effect decoupled from reactivity, and explains how it is possible to modulate reactivity without changing affinity. Such decoupling clearly is of physiological relevance for the reduction of met-Mb in muscle and of met-Hb in a red cell, where tight binding of cyt b_5 to the high concentration of ferrous-Mb/Hb would prevent the cytochrome from finding and reducing the oxidized proteins; it likely is of physiological relevance in other situations, as well.

Materials and Methods

Materials. Myoglobin (horse heart) was purchased from Sigma. The trypsin-solubilized cytochrome b_5 (bovine) was expressed and purified according to the procedures described by Mauk and co-workers.[15] Deuteroporphyrin IX was purchased from Frontier Scientific.

Synthesis of Zinc-deuteroporphyrin IX Dimethylester. Two hundred milligrams of deuteroporphyrin IX was added to 30 mL of 5% (w/v) $H_2SO_4-CH_3OH$, and the reaction mixture was stirred at 4 °C in the dark for 24 h. The methylated deuteroporphyrin was extracted into ether and readily purified by chromatography on silica gel with ethyl acetate as eluent (yield > 90%).

To a boiling chloroform solution containing 150 mg of the methylated deuteroporphyrin prepared above was added 20 mL of a saturated solution of zinc acetate in methanol. The reaction mixture was refluxed in the dark for about 30 min, and the completion of zinc-(II) insertion was indicated by the UV−vis spectrum. Filtration of the reaction mixture gave ~140 mg of red precipitate as the final product. ^1H NMR (300 MHz, $CDCl_3$): δ 3.05 (m, 4H), 3.27−3.67 (m, 18H), 4.32 (t, 4H), 6.90 (s, 2H), 7.60 (s, 2H), 8.66 (d, 2H), 9.09−9.12 (m, 4H).

Synthesis of Zinc-deuteroporphyrin IX Diamide. In situ preparation of aluminum amide reagent for the transformation of ester to amide: To a suspension of NH_4Cl (0.01 mol, 550 mg) in 10 mL of dry benzene at 4 °C was slowly added 5 mL of a toluene solution of trimethyl aluminum (2 M). After the addition was completed, the reaction mixture was allowed to warm to room temperature and was stirred for about 2 h until gas evolution had ceased.[16,17]

Two milliliters (1.2 mmol) of this aluminum amide reagent was then added to a solution of the zinc-deuteroporphyrin IX dimethylester (0.2 mmol, 140 mg) in 4 mL of dry benzene. The solution was warmed to 45 °C under nitrogen protection in the dark until no starting ester was observed by TLC (~20 h). After being cooled to room temperature, the product was precipitated by quenching with 2 mL of 5% HCl,

(8) Liang, Z.-X.; Jiang, M.; Ning, Q.; Hoffman, B. M. *J. Biol. Inorg. Chem.* **2002**, in press.
(9) Naito, N.; Huang, H.; Sturgess, W.; Nocek, J. M.; Hoffman, B. M. *J. Am. Chem. Soc.* **1998**, *120*, 11256−11262.
(10) Naito, A.; Hui, H. L.; Noble, R. W.; Hoffman, B. M. *Biochemistry* **2001**, *40*, 2060−2065.
(11) Nocek, J. M.; Sishta, B. P.; Cameron, J. C.; Mauk, A. G.; Hoffman, B. M. *J. Am. Chem. Soc.* **1997**, *119*, 2146−2155.
(12) McLachlan, S. J.; La Mar, G. N.; Sletten, E. *J. Am. Chem. Soc.* **1986**, *108*, 1285−1291.
(13) Hunter, C. L.; Lloyd, E.; Eltis, L. D.; Rafferty, S. P.; Lee, H.; Smith, M.; Mauk, A. G. *Biochemistry* **1997**, *36*, 1010−1017.
(14) Liang, Z.-X.; Nocek, J. M.; Kurnikov, I. V.; Beratan, D. N.; Hoffman, B. M. *J. Am. Chem. Soc.* **2000**, *122*, 3552−3553.
(15) Funk, W. D.; Lo, T. P.; Mauk, M. R.; Brayer, G. D.; MacGillivray, R. T. A.; Mauk, A. G. *Biochemistry* **1990**, *29*, 5500−5508.
(16) Basha, A.; Lipton, M.; Weinreb, S. M. *Tetrahedron Lett.* **1977**, 4171−4174.
(17) Levin, J. I.; Turos, E.; Weinreb, S. M. *Synth. Commun.* **1982**, *12*, 989−993.

collected by vacuum filtration, and purified by silica gel column chromatography. The desired product eluted as a red band with methanol as eluent after the remaining starting material and byproducts were eluted with CH_2Cl_2 and ethyl acetate. Removal of the solvent by evaporation gave 90 mg (60%) of the product. ^{1}H NMR (500 MHz, DMSO): δ 3.04 (t, 4H), 3.60−3.74 (m, 12H), 4.32 (t, 4H), 6.90 (s, 2H), 7.60 (s, 2H), 9.22 (d, 2H), 10.05−10.23 (m, 4H). ^{13}C NMR: δ 12.11, 14.13, 22.93, 97.83, 100.57, 101.31, 130.25, 137.26, 141.09, 147.69, 148.19, 148.81, 174.89. MS (EI): 571.4.

Synthesis of Zinc-deuteroporphyrin IX ^{15}N-Diamide. The procedure was the same as that used to prepare zinc-deuteroporphyrin IX diamide, except the aluminum amide reagent was prepared using $^{15}NH_4Cl$. ^{1}H NMR (500 MHz, DMSO): δ 3.04 (t, 4H), 3.60−3.74 (m, 12H), 4.32 (t, 4H), 6.77−7.76 (q, 4H), 9.22 (d, 2H), 10.05−10.23 (m, 4H). ^{13}C NMR: δ 12.11, 14.13, 22.93, 97.83, 100.57, 101.31, 130.25, 137.26, 141.09, 147.69, 148.19, 148.81, 174.89. MS (EI): 573.3.

Preparation of Zinc-Substituted Mb's. ZnMb was prepared with the procedure we described previously.[11] ZnMb(dme), ZnMb(diamide), and ZnMb(^{15}N-diamide) were prepared with a modified procedure described here. First, apoMb was prepared using the method of Teale[18] and dialyzed against 25 mM, pH 6.0 KPi buffer overnight. A 1.5-fold molar excess of one of the zinc-porphyrins, either the ester or the amide, was dissolved in a warm CH_3OH/DMSO (3:1 v/v) solution. After being cooled to 4 °C, the porphyrin solution was added dropwise to the apoMb solution with stirring at 4 °C, and the protein solution was kept in the dark at 4 °C for 2 h. A second 1.5-fold molar excess of porphyrin was then added in the same fashion, and the solution was kept at 4 °C for another 2 h. The progress of the reconstitution process was followed by monitoring the formation of the 414 nm absorption band of the product in the UV−vis spectrum. In the reconstitution process, the total volume of the organic solution added into the protein solution was kept below 8% percent of the apo-Mb solution to prevent protein denaturation. Following dialysis against phosphate buffer (pH 6.0, 25 mM) overnight, the protein solution was concentrated and loaded onto a Sephadex G-25 column to remove remaining free porphyrin. The protein was further purified by HPLC with a TSK-based cation-exchange column (Beckman, 21.5 mm × 15 cm, SP-5PW) and a 25 mM KPi pH gradient (pH range, 6.0−12.0).

Kinetics Measurements. Proteins were exchanged into working buffer using Centricon microconcentrators (Amicon). Anaerobicity was achieved by bubbling nitrogen through buffer solution in a sealed cuvette for an hour, and gently purging the protein stock solution with nitrogen for 20 min prior to addition to the sample cuvette. Kinetic measurements were performed on two previously described laser flash photolysis apparatus. The majority employed an apparatus with a time constant of 15 μs and a continuous tungsten lamp as probe light source;[11] the most rapid reactions were monitored on an apparatus with a time constant of a few nanoseconds and a xenon flash lamp as probe light source.[19,20]

Isothermal Titration Calorimetry. Isothermal titration calorimetry (ITC) experiments were performed on an OMEGA titration microcalorimeter from MicroCal, Inc. The proteins were exchanged into desired buffer by dialysis against 4 L of 10 mM, pH 6.0 KPi buffer overnight at 4 °C, and degassed using a vacuum pump. The titration was carried out by adding a ZnMb or ZnMb(dme) solution into a cyt b_5 solution (~0.3 mM) at 20 °C. The baseline was corrected by subtracting the data from the titration of protein solutions into buffer. The final data were analyzed using the program ORIGIN (MicroCal, Inc.) incorporating equations for one-site binding.

NMR Experiment. The protein samples were prepared by dialysis against 4 L of 10 mM, pH 6.0 KPi overnight at 4 °C. The [^{1}H, ^{15}N]-HSQC spectrum was acquired at 20 °C on a Varian INOVA spectrometer equipped with a 5 mm triple resonance gradient probe using 128 × 512 complex points and spectral width of 365 × 8000 Hz in the $d_1 \times d_2$ dimensions. The 2D ^{15}N-edited [^{1}H, ^{1}H]-NOESY-HSQC spectrum with a mixing time of 150 ms was acquired using 128 × 512 complex points and spectral width of 6001 × 6001 Hz in the $d_1 \times d_2$ dimensions. The data were processed using Felix 97 (MSI, San Diego). A sinebell window function was applied in both d_1 and d_2 dimensions. The spectra were zero-filled to give a final matrix size of 256 × 1024. Chemical shifts were referenced to the water peak at 4.64 ppm.

Electron-Transfer Pathway Analysis. The principles of ET pathway analysis are based on the approximate method PATHWAY introduced by Beratan and Onuchic et al.[21] Electronic couplings in the PATHWAY model were computed as a product of decay factors associated with covalent bonds (ϵ_{bond}), nonbonded contacts (ϵ_{nb}), and hydrogen bonds (ϵ_{hb}) between atoms on a path from the donor to the acceptor atom. Electronic coupling maps were generated by calculating the electronic tunneling matrix element from the redox cofactors in the protein to each atom on the protein surface.[22,23]

Brownian Dynamic (BD) Simulation. BD simulations were performed with the Macrodox program developed by Northrup and coworkers at Tennessee Tech. The details of BD simulation of protein−protein interaction have been described elsewhere.[24,25] Briefly, the X-ray crystallographic coordinates of ferri-Mb (1YMB) and cyt ferri-b_5 (1CYO) were downloaded from the protein data bank, and the coordinates for ZnMb and ZnMb(dme) were generated in WebLab (MSN) by replacing the iron atom of the Mb coordinates with zinc atom and adding two methyl groups to the propionates for ZnMb(dme). The coordinates for the tryptic cyt b_5 were generated by deleting the terminal residues flanking the tryptic fragment. In the program, charges are assigned on the basis of the pK_a values estimated by Tanford−Kirkwood calculation. On the basis of those assigned charges, a Poisson−Boltzmann calculation is performed to determine the electrostatic potential grid surrounding ZnMb. In the simulation, cyt b_5 is simply treated as an array of test charges in the field of ZnMb without considering its internal low dielectric. The simulation starts with the center of cyt b_5 70 Å away from the ZnMb potential grid. The Brownian motion of cyt b_5 in the field of ZnMb was simulated stochastically by a series of small displacements governed by the Smoluchowski diffusion equation with forces. A trajectory would be declared to be successful if the distance between any meso carbon (C_M) of one heme reaches a prescribed distance from any C_M of the partner heme at any time before cyt b_5 passes outside an escape radius of 200 Å. For each successful trajectory, the position of cyt b_5 at the instant of contact with the surface of ZnMb is recorded, although the trajectories were not truncated until the outer 200 Å sphere was reached.[26] For ZnMb, the simulation with 10 000 trajectories under the condition of pH 7.0, 18 mM ionic strength (10 mM KPi buffer) took 3 h of CPU time (SGI O_2), while the simulation took 20 h for Zn(dme)Mb. A simulation generated a large set of complexes, and they are represented here as a so-called docking profile in which the centers of mass of cyt b_5 in each complex are represented as yellow dots surrounding ZnMb or ZnMb(dme).

Results

ET Kinetics. The three zinc deuteroporphyrin-substituted ZnMb's (Figure 1) have virtually identical UV−vis spectra, with

(18) Teale, F. W. J. *Biochim. Biophys. Acta* **1959**, *35*, 543.
(19) Greenfield, S. R.; Svec, W. A.; Gosztola, D.; Wasielewski, M. R. *J. Am. Chem. Soc.* **1996**, *118*, 6767−6777.
(20) We thank Prof. M. Wasielewski for the use of this apparatus.
(21) Beratan, D. N.; Onuchic, J. N.; Winkler, J. R.; Gray, H. B. *Science* **1992**, *258*, 1740−1741.
(22) Nocek, J. M.; Zhou, J. S.; De Forest, S.; Priyadarshy, S.; Beratan, D. N.; Onuchic, J. N.; Hoffman, B. M. *Chem. Rev.* **1996**, *96*, 2459−2489.
(23) Roitberg, E. A.; Holden, M. J.; Mayhew, M. P.; Kurnikov, I. V.; Beratan, D. N.; Vilker, V. L. *J. Am. Chem. Soc.* **1998**, *120*, 8927−8932.
(24) Northrup, S. H.; Boles, J. O.; Reynolds, J. C. L. *Science* **1988**, *241*, 67−70.
(25) Northrup, S. H.; Thomasson, K. A.; Miller, C. M.; Barker, P. D.; Eltis, L. D.; Guillemette, J. G.; Inglis, S. C.; Mauk, A. G. *Biochemistry* **1993**, *32*, 6613−6623.
(26) Thus, the distance of closest approach for a trajectory with a particular target distance could be less than that value.

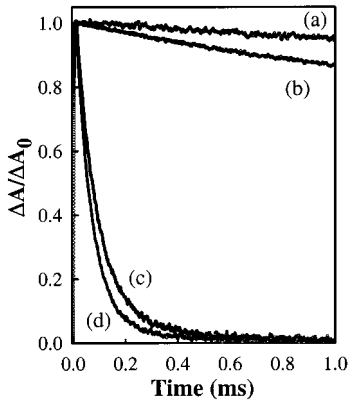

Figure 2. Triplet decay traces for (a) ZnMb (5 μM), $k_{obs} = 52\ s^{-1}$; (b) ZnMb (5 μM) + cyt b_5 (10 μM), $k_{obs} = 113\ s^{-1}$; (c) ZnMb(dme) (5 μM) + cyt b_5 (10 μM), $k_{obs} = 5.5 \times 10^3\ s^{-1}$; and (d) ZnMb(diamide) (5 μM) + cyt b_5 (10 μM), $k_{obs} = 7.9 \times 10^3\ s^{-1}$. Conditions: 10 mM potassium phosphate buffer at pH 7.0, 20 °C.

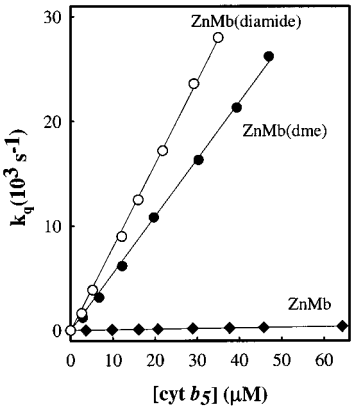

Figure 3. Triplet quenching plots for ZnMb (slope, $k_2 = 6.1 \times 10^6\ M^{-1}\ s^{-1}$), ZnMb(dme) (slope, $k_2 = 5.5 \times 10^8\ M^{-1}\ s^{-1}$), and ZnMb(diamide) (slope, $k_2 = 7.9 \times 10^8\ M^{-1}\ s^{-1}$) (~5 μM each) upon addition of cyt b_5. Conditions: 10 mM potassium phosphate buffer at pH 7.0, 20 °C.

Soret maxima at 414 nm, and α- and β-bands at 542 and 580 nm; all have identical triplet decay rate constants of $k_d = 52 \pm 2\ s^{-1}$ as monitored by transient-absorption spectroscopy. Photoinduced ET between the ZnMb's and (Fe^{3+})cyt b_5 was monitored spectroscopically as quenching of the excited triplet state of the ZnMb's. In the presence of cyt b_5, the triplet decays remain exponential, but the decay rate constants for all three ZnMb's, denoted k_{obs}, are increased by ET quenching, with a quenching constant of $k_q = k_{obs} - k_d$. This indicates that the reaction between the Mb's and cyt b_5 is in the rapid-exchange limit, as discussed previously.[11] The quenching of these ZnMb's by cyt b_5 was confirmed to involve ET through observation of the time-resolved signals from the intermediate produced by photoinitiated ET, the long-lived zinc porphyrin radical cation characterized by a peak at 670 nm, and the reduced cyt b_5, by a peak at 562 nm. However, the signals for **2** and **3** are much weaker and more difficult to detect than those for **1** (data not shown), presumably because the rate constant for the return of the intermediate to the ground state is much greater (see below.)

Experiments at a fixed cyt b_5 concentration show that the quenching rates for the two charge-neutralized proteins, ZnMb(dme) and ZnMb(diamide), are much greater than that of ZnMb. For example, at pH 7.0 and 10 mM KPi, a 2-fold excess of cyt b_5 gives a quenching rate constant for ZnMb (5 μM) of $k_q = 61\ s^{-1}$, while k_q for the charge-neutralized ZnMb(dme) and ZnMb(diamide) is 2 orders of magnitude greater, $k_q = 5.5 \times 10^3\ s^{-1}$ and $7.9 \times 10^3\ s^{-1}$ (Figure 2), respectively. The quenching constants k_q for all three ZnMb's increase linearly with increasing cyt b_5 concentration, and none showed any sign of saturation over the course of a titration in which cyt b_5 reaches a concentration of ~50 mM, consistent with the binding constants given below (Figure 3). The plots of k_q versus [cyt b_5] yielded bimolecular quenching rate constants (k_2), as follows: k_2 (ZnMb) $= 6.1 \times 10^6\ M^{-1}\ s^{-1}$, k_2 (ZnMb(dme)) $= 5.5 \times 10^8\ M^{-1}\ s^{-1}$, and k_2 (ZnMb(diamide)) $= 7.9 \times 10^8\ M^{-1}\ s^{-1}$. The rate constants for the charge-neutralized ZnMb(dme) and ZnMb(diamide) thus are 90- and 130-fold greater than that of ZnMb, respectively, under these conditions. The ~50% difference between the rate constants for ZnMb(dme) and ZnMb(diamide), though small, is reproducible.

Measurements of the bimolecular rate constants k_2 at different pH values accentuate the remarkable difference between ZnMb and ZnMb(dme). The k_2 for ZnMb decreases ~30-fold as the pH is raised from 6.0 to 8.0, whereas that for ZnMb(dme) decreases only ~3-fold over the same pH range. As a result, the enhancement of k_2 by ester charge neutralization ranges from 250-fold at pH 8.0 down to 30-fold at pH 6.0 (Table 1).

Table 1. pH Dependence of Quenching Rate Constants (k_2) for ZnMb and ZnMb(dme)[a]

pH	k_2 ($M^{-1}\ s^{-1}$)		k(ZnMb(dme))/ k(ZnMb)
	ZnMb	ZnMb(dme)	
6.0	4.4×10^7	1.2×10^9	27
6.3	2.5×10^7	1.0×10^9	40
6.5	1.7×10^7	7.7×10^8	45
7.0	6.1×10^6	5.5×10^8	90
7.3	5.0×10^6	4.9×10^8	98
7.5	3.1×10^6	4.6×10^8	148
8.0	1.7×10^6	4.3×10^8	253

[a] Conditions: 10 mM potassium phosphate buffer, 20 °C.

Charge neutralization not only enhances the quenching rate at all pH values; it also enhances the sensitivity of k_2 to ionic strength. As shown in Figure 4, the quenching constant for ZnMb at pH 7.0 decreases minimally with increasing NaCl salt concentration, dropping by less than one-half as the salt concentration is increased from 1 to 400 mM. In contrast, k_2 for ZnMb(dme) drops by one-half at less than 20 mM salt, and is reduced by 2 orders of magnitude by 400 mM salt.

Binding Constant Measurements. Cyt b_5 binds to ZnMb with an affinity constant, $K_a = 10^3\ M^{-1}$,[27] as measured in an NMR titration. With such a low affinity, quenching titrations at the protein concentrations employed here do not show signs of saturation, Figure 2. The fact that the quenching titration curves for ZnMb(dme) and ZnMb(diamide) also do not show saturation suggests that the affinity of Mb for cyt b_5 is not enhanced substantially by charge neutralization; modeling shows that an increase in the binding constant by more than 3−4-fold would cause the titrations to show curvature, counter to experiment. The actual changes in affinity were determined by use of isothermal titration calorimetry (ITC) and by NMR titrations (see below) to measure the binding of cyt b_5 to ZnMb and ZnMb(dme). Heats produced during ITC titrations of cyt b_5 by ZnMb and ZnMb(dme) at pH 7.0 were too small to allow determination of binding constants, but could be used to measure

(27) Liang, Z.-X. Ph.D. Thesis; Northwestern University: Evanston, IL, 2001.

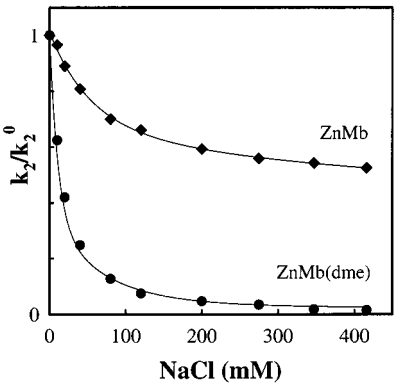

Figure 4. Ionic strength dependence of the cyt b_5 quenching of photoexcited ZnMb and ZnMb(dme). The quenching constant was measured for each at fixed concentration of the Mb (~5 μM) and cyt b_5 (~10 μM) as NaCl was added. The quenching constants are normalized to that at the initial ionic strength (18 mM); see caption to Figure 2. As a result, the plotted values correspond to the relative values of k_2. Conditions: pH 7.0, 10 mM potassium phosphate buffer at 20 °C.

the affinities at pH 6.0. Figure 5 presents the results of ITC titrations carried out when ZnMb or ZnMb(dme) solutions (10 mM KPi buffer at pH 6.0) were added to a cyt b_5 solution (0.4 mM). The heats released during the course of the titration were fit to a one-site binding model, which yielded the affinity constants, $K_a = 350 \pm 65$ and 540 ± 70 M^{-1} for ZnMb/cyt b_5 and ZnMb(dme)/cyt b_5, respectively; the former value is consistent with that measured previously by an NMR titration.[8,27] Thus, the charge neutralization in fact does not significantly alter the thermodynamic binding constant, despite its profound effect on ET reactivity.

NMR Studies. We prepared ZnMb(^{15}N-diamide) to enable us to use 2D NMR techniques to study protein recognition and to obtain an independent measure of binding affinity. The [^{1}H,^{15}N]- HSQC spectrum (not shown) of the free zinc deuteroporphyrin IX ^{15}N-diamide in DMSO shows two resonances corresponding to the syn and anti protons of the two amides. The [^{1}H,^{15}N]-HSQC spectrum of the ZnMb(^{15}N-diamide) (Figure 6) shows two sets of four peaks. The two sets are assigned to two Mb conformers (^{15}N-H1, H2, H3, H4 and ^{15}N-H1′, H2′, H3′, and H4′) that differ by a 180° degree rotation of the porphyrin ring along its α-γ-meso axis, as seen in native Mb. The appearance of four peaks per conformer indicates that the environments of the two propionamides differ. The ratio of the intensities of the two sets of peaks indicates that the two conformers are in a 3:2 ratio. Native Mb also exhibits two such conformers, but with a ratio of 9:1.

The ^{15}N-edited [^{1}H−^{1}H]-NOESY-HSQC spectrum of ZnMb-(diamide), Figure 6 (bottom), has NOE cross-peaks that correlate the two amide protons of one propionamide of each conformer (1, 2; 3′, 4′) to protons of a protein residue(s), which implies that this propionamide is held in a stable configuration, in close contact with protons of that residue. This residue is tentatively assigned as Ser92, on the basis of the distinctive chemical shifts of the two β-H of serine (~3.6 ppm) and the proximity of Ser92 to one of the propionates in the Mb structure. This suggests that in each conformer of **4**, this propionamide is hydrogen bonded to and fixed in the protein pocket, while the other sticks out of the heme pocket and is exposed to the solvent, just as do the propionates in native Mb.[13,28,29]

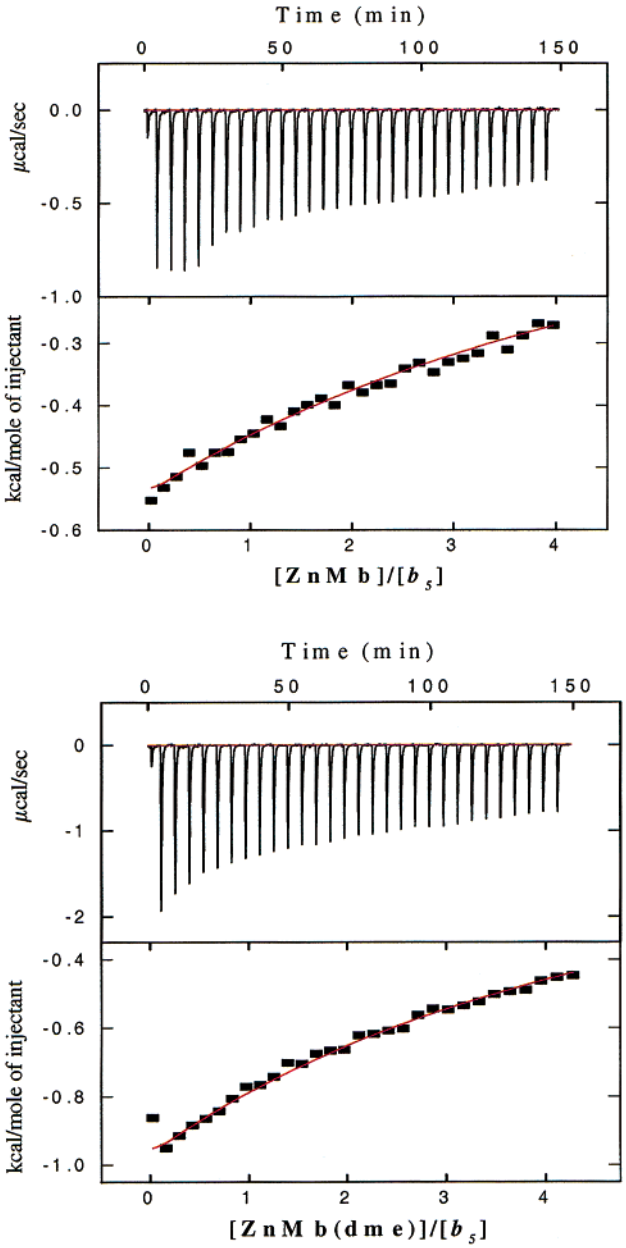

Figure 5. Binding affinity between cyt b_5 and ZnMb/ZnMb(dme) as measured by isotherm titration calorimetry (ITC). Aliquots of ZnMb or ZnMb(dme) were titrated into the cyt b_5 (~0.3 mM) solution. The raw data are shown in the upper panels, and the integrated, baseline-corrected data are shown in the lower panels. Fitting of the data to an 1:1 binding model gives the curves shown, with binding constants $K_a = 350$ (±)65 M^{-1} and 540 (±)70 M^{-1} for ZnMb/cyt b_5 and ZnMb(dme)/cyt b_5, respectively. Conditions: 10 mM potassium phosphate buffer at pH 6.0, 20 °C.

Addition of cyt b_5 to a solution of **4** causes a progressive downfield shift of the four peaks in the HSQC spectrum (H1′, H2′; H3, H4; most notably H1′ and H4) that are associated with the solvent-exposed propionate of each conformer (Figure 7). The NMR titration curves in Figure 7 have been fit to a 1:1 binding model, as shown in the figure. The fits yielded $K_a \approx 500-1000$ M^{-1} for cyt b_5/ZnMb(diamide), consistent with the results of isothermal calorimetry.

(28) La Mar, G. N.; Emerson, S. D.; Lecomte, J. T. J.; Pande, U.; Smith, K. M.; Craig, G. W.; Kehres, L. A. *J. Am. Chem. Soc.* **1986**, *108*, 5568−5573.
(29) Lloyd, E.; King, b. B. C.; Hawkridge, F. M.; Mauk, A. G. *Inorg. Chem.* **1998**, *37*, 2888−2892.

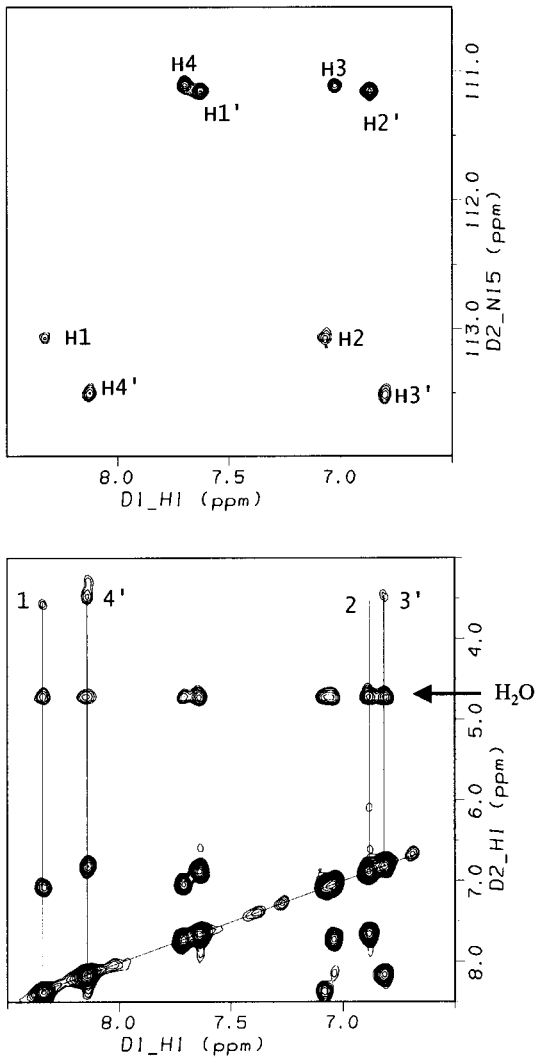

Figure 6. (Top) [^{1}H,^{15}N]-HSQC spectrum of ZnMb(^{15}N-diamide) showing four amide proton peaks for each of the two conformers. (Bottom) [^{1}H,^{1}H]-NOESY-HSQC spectrum, which shows NOE cross-peaks between protein residue, possibly the β-H of Ser92, and amide protons H1, H4′, H2, H3′. Conditions: pH 6.0, 10 mM KPi, 20 °C.

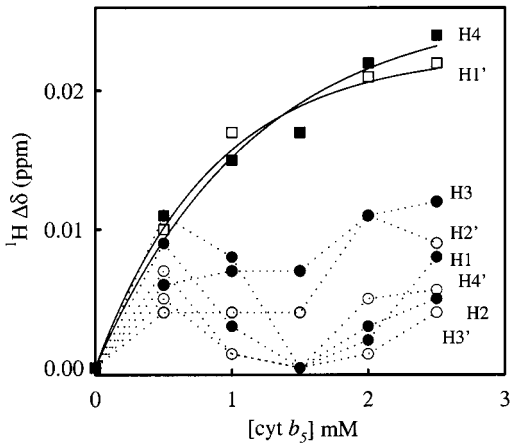

Figure 7. Normalized ^{1}H chemical shift changes caused by the titration of ZnMb(^{15}N-diamide) with cyt b_5. [ZnMb(^{15}N-diamide)] = 0.9 mM. Conditions: pH 6.0, 10 mM KPi, 20 °C. The smooth lines through the points for H4 (■) and H1′ (□) are the fits to single binding isotherms with K_a in the range of 500−1000 M^{-1}.

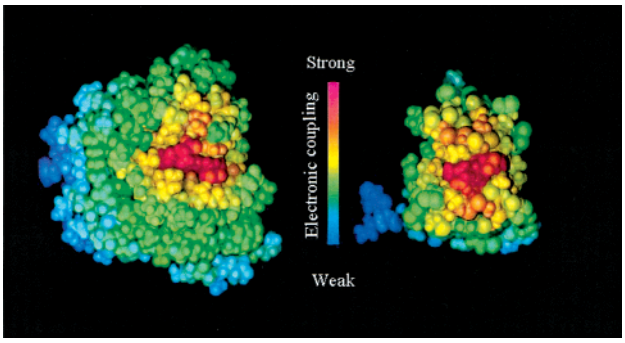

Figure 8. Electronic coupling maps for Mb (left) and cyt b_5 (right) from electron-transfer pathway calculation. The surface area with strong coupling to the redox center is shown in red and is the reactive surface for ET.

Electron-Transfer Pathway Analysis. ET pathway calculations were carried out to identify the surface residues or atoms that have large electronic couplings to the redox centers in their respective proteins. The electronic coupling maps (Figure 8) generated by ET pathway calculations show the relative couplings projected onto the surface of Mb and cyt b_5; the coloring is proportional to the logarithm of the square of the coupling from the surface atom to its redox center, red representing larger coupling and blue representing smaller. These coupling maps show that for both proteins there is only a small "ET-active" region with relatively large couplings and that this includes only the exposed heme edge and its close vicinity. Of particular importance, this "active" region for Mb is essentially unchanged by charge neutralization. Indeed, the additional steric bulk of the methyl groups which lengthens the ET pathway between partner hemes would, at most, slightly weaken the coupling between the Mb surface and its heme.

Brownian Dynamic (BD) Simulations. BD simulations were performed to study the electrostatically controlled diffusion and docking of cyt b_5 with ZnMb (**1**) and ZnMb(dme) (**2**). With the pH set to 7.0 and ionic strength to 18 mM (10 mM KPi), a 10 000-trajectory run with **1** or **2** generated the so-called docking profiles shown in Figure 9. In the docking profiles, **1** and **2** are represented by the solid ribbon, and the centers of mass of successfully docked cyt b_5 are represented by the yellow dots; the criterion for productive docking is that the distance between meso carbons on the two porphyrin rings reaches 25 Å (see Materials and Methods). The success rate of docking is not sharply altered by charge neutralization, as might be expected from the small experimental effect on affinity: for ZnMb, 2573 docked complexes were generated from 10 000 trajectories (Figure 9, top), as compared with 3629 complexes generated for ZnMb(dme) (Figure 9, bottom).

However, the distribution of "hits" is sharply altered. The cyt b_5 dots scatter almost uniformly over the ZnMb surface. A separate calculation of 10 000 trajectories for ZnMb/cyt b_5 with the distance criterion set to be less than 10 Å showed fewer than 10 "hits". In contrast, for ZnMb(dme)/cyt b_5, the hits are much more densely populated around the porphyrin edge. There is a striking increase in the number of the complexes with short heme−heme distance; a separate calculation showed ∼1400 hits with a criterion of 10 Å or less.

Contact-frequency histograms (Figure 10) show the frequency with which the individual charged surface residues of ZnMb and ZnMb(dme) are involved in close ionic contacts within the encounter complexes found by the Brownian dynamics simulations (for 18 mM ionic strength; 25 Å distance criterion). The

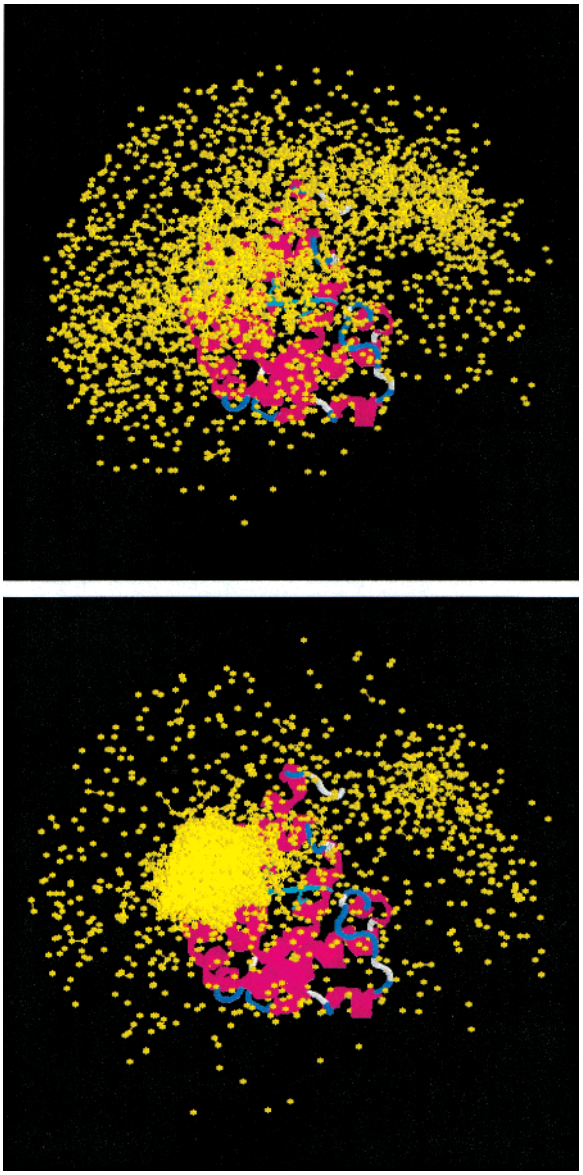

Figure 9. Docking profiles for the docking of cyt b_5 onto ZnMb (top) and ZnMb(dme) (bottom). The solid ribbon structures in the middle represent ZnMb and ZnMb(dme) respectively, and the yellow dots represent the centers of mass of the incoming cyt b_5 at the point the distance criterion, a 25 Å C_M-C_M distance in this case, is met. Conditions of BD simulation are set as 10 000 trajectories, pH 7.0, 18 mM ionic strength (10 mM KPi), 20 °C.

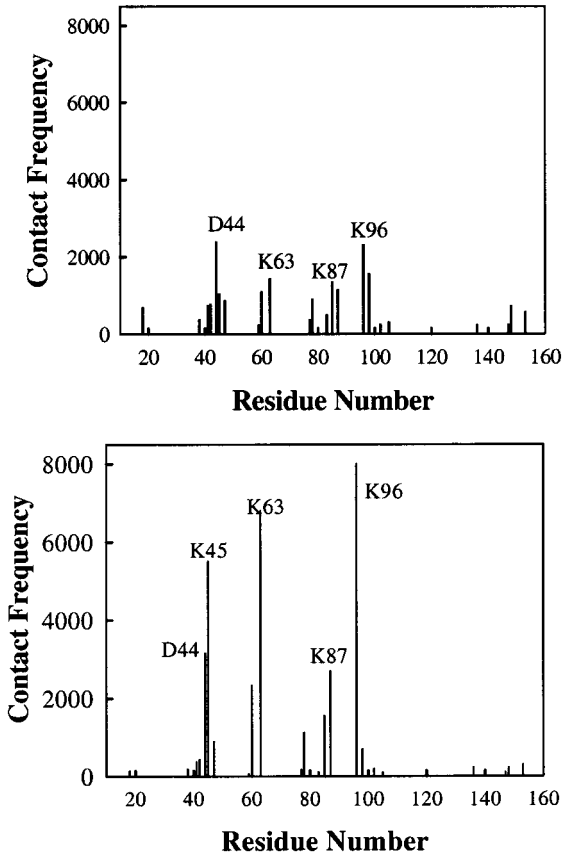

Figure 10. Contact histograms of frequencies showing the charged residues of ZnMb (top) and ZnMb(dme) (bottom) involved in ionic contacts with cyt b_5 residues. The total number of contacts for each formally charged residue is an indication of the importance of an individual residue in forming the protein complex for ET.

histograms show that charge neutralization of the heme propionate of Mb greatly increases the probability for the heme itself and the charged residues surrounding the Mb heme edge, Lys 45, Lys 63, Lys 96, to make contact with the incoming cyt b_5.

BD simulations also were carried out for pH 7.0 and an ionic strength of 200 mM. Under these conditions, the docking profiles for ZnMb and ZnMb(dme) are very similar (not shown), with a broad docking surface for both proteins. Thus, in agreement with our experiments, the favorable electrostatic effects of charge neutralization appear to be "screened" away at high ionic strength.

Analysis and Discussion

Cyt b_5 binds weakly to Mb, and we initiated these studies with the hypothesis that the elimination of the two negative charges on the ZnMb surface would "tighten" the complex by enhancing the electrostatic attraction of Mb for the negatively charged cyt b_5. Surprisingly, the neutralization did not lead to evidence of saturation in titrations of ZnMb(dme), suggesting that the binding is not substantially enhanced by charge neutralization, yet it caused a dramatic increase in k_2.[14] In this report, we have explored this finding.

The NMR and optical spectroscopic studies provide a foundation for interpreting the ET quenching results, by confirming that reconstitution of Mb with propionate-neutralized zinc porphyrin causes minimal structural perturbation. The optical properties of both ZnMb(dme) and ZnMb(diamide) are indistinguishable from those of ZnMb. Heteronuclear NMR spectra of the ZnMb(^{15}N-diamide) (Figure 6, top) show that the zinc-deuteroporphyrin(^{15}N-diamide) remains locked into the Mb heme pocket, with two conformations in equilibrium as in native Mb. La Mar and co-workers have shown that the two conformers differ by a 180° rotation along the heme α-γ-meso axis.[28] The ratio of the two conformers is 9:1 for native Mb, but 3:2 for ZnMb(diamide). This difference is attributed to the replacement of the bulky peripheral vinyl groups by hydrogens, rather than to a consequence of methylating the propionates.[30] In addition, [^{1}H,^{1}H]-NOESY-HSQC experiments (Figure 6, bottom) suggest that one propionate of ZnMb(diamide) is hydrogen-bonded to protein residues, presumably Lys45, Ser92, and His97, while

(30) Neya, S.; Funasaki, N.; Igarashi, N.; Ikezaki, A.; Sato, T.; Imai, K.; Tanaka, N. *Biochemistry* **1998**, *37*, 5487−5493.

the other is flexible and exposed to solution, just as is found in native horse Mb.[28,29]

We have explored how neutralization of the Mb heme propionates affects ET with cyt b_5, studying two Mb derivatives over a wide range of pH values and ionic strengths. Neutralization dramatically increases the second-order ET rate constant: k_2 for ZnMb(dme) is ~100-fold greater than that for ZnMb at pH 7, and ~250-fold greater at pH 8. We further introduced the porphyrin diamide as a new means of neutralizing the propionates, one which introduces a hydrophilic, not hydrophobic, surface moiety. There is an additional small increase of ca. 1.5-fold in k_2 for the ZnMb(diamide), as compared to ZnMb(dme). This small difference most likely arises because the bulkier methyl groups sterically hinder cyt b_5 from approaching the porphyrin edge of ZnMb(dme), and thereby diminish the electronic coupling for ET. Our discussion will focus on the large differences between the ET rates for ZnMb and ZnMb(dme).

Although heme neutralization causes a dramatic increase in k_2, it does not cause a significant increase in the thermodynamic binding constant. This is indicated by the fact that neither ZnMb(dme) nor ZnMb(diamide) show binding saturation with cyt b_5 at concentrations of $\lesssim 100\ \mu$M. It is demonstrated quantitatively by ITC measurements which show that the affinities of cyt b_5 for ZnMb and ZnMb(dme) differ minimally, with $K_a \approx 300-500\ M^{-1}$ for both at pH 6.0 (Figure 5). This result is obtained independently through the NMR titrations, which give $K_a \approx 500-1000\ M^{-1}$ for the binding of cyt b_5 to both ZnMb[8] and ZnMb(diamide) (Figure 7).[31,32] Thus, the increase in the second-order rate constant k_2 upon neutralization of the Mb propionates is not caused by tighter binding.

"Simple Docking" (SD) Model. Can the effects of charge neutralization on ET between Mb and cyt b_5 be understood within the "simple docking" model whose "energy landscape"[33] is sketched in Figure 11? In this model, as formulated in the kinetic equations of eq 1a, ZnMb and cyt b_5 bind to form a single well-defined complex, with association and dissociation rate constants, k_{on} and k_{off}, binding constant, $K_a = k_{on}/k_{off}$, and an intracomplex ET rate constant, k_{et}.[11]

$$*\mathrm{ZnMb} + (\mathrm{Fe}^{3+})\mathrm{cyt}\ b_5 \underset{k_{off}}{\overset{k_{on}}{\rightleftharpoons}} *\mathrm{ZnMb}/(\mathrm{Fe}^{3+})\mathrm{cyt}\ b_5 \xrightarrow{k_{et}} \mathrm{Zn}^{+}\mathrm{Mb}/(\mathrm{Fe}^{2+})\mathrm{cyt}\ b_5 \quad (1a)$$

When the concentrations of the two reacting proteins are small as compared to the inverse of the binding constant, as in our ET measurements, the triplet-state ET quenching is characterized by a steady-state bimolecular ET rate constant, $k_2 = k_{et} \times k_{on}/(k_{off} + k_{et})$. We now show that, as suggested earlier,[11] our experiments involve the fast-exchange, or "reaction", limit in which $k_{off} \gg k_{et}$ in the SD model. First, as previously noted, failure of this limit likely would lead to triplet decays that are not monoexponential.[11] Second, the dramatic change in k_2 with charge neutralization is not compatible with the opposite (diffusion) limit in which $k_{off} \ll k_{et}$, where the quenching constant becomes $k_2 = k_{on}$. In this limit, the dependence of k_2 on Mb charge must be linear or less,[34] whereas the experimental variation of k_2 with charge is far stronger.[35] Finally, direct estimation indicates the reaction limit. From the binding constant, $K_a = k_{on}/k_{off} \lesssim 10^3\ M^{-1}$, and the use of a reasonable value, $k_{on} \gtrsim 10^9\ M^{-1}\ s^{-1}$, as estimated from the protein−protein diffusion constant, one gets $k_{off} \gtrsim 10^6\ s^{-1}$. The electron-transfer rate constant, k_{et}, can be estimated using pathway-based analysis of the protein-mediated coupling.[21] The protein−protein configurations with the strongest donor−acceptor interactions have coupling pathways through a propionate from each of the partner hemes, linked by a nonbonded contact. The decay of coupling across the propionate of one heme is ~10 (because each of the 3−4 propionate bonds has a decay factor of 0.6), or 10^2 for the two. A nonbonded step of 3−4 Å produces a coupling decay of $\sim 10^2$. The result is a decrease of the ET coupling, relative to direct heme-to-heme contact, of $\sim 10^4$. The rate constant k_{et} depends on the square of the coupling, and thus will decrease by $\sim 10^8$. Assuming that activationless ET between two hemes in direct contact has a rate constant of $\sim 10^{12}-10^{13}\ s^{-1}$, we thus crudely estimate the activationless (maximum) intracomplex ET rate constant to be $k_{et} \approx 10^4-10^5\ s^{-1}$, 1−2 orders of magnitude less than the estimated value of k_{off}. In the resulting reaction limit, the second-order ET quenching constant for the SD model thus becomes the product of k_{et} and the thermodynamic binding constant, K_a (eq 1b).

$$k_2 = k_{et} \times K_a \quad (1b)$$

Within the model of eq 1, the difference between the second-order quenching rate constants for ZnMb and its charge-neutralized variants ZnMb(dme) and ZnMb(diamide) could, in principle, arise from increases in k_{et}, K_a, or both (eq 1b). As our experiments show that K_a does not change appreciably, then *within this model* the differences could only reflect changes in k_{et}. However, we now show that this cannot be the case either.

An intracomplex ET rate constant k_{et} is the product of an electronic coupling term and a Franck−Condon overlap factor associated with nuclear reorganization.[36] The large increase in k_2 upon heme neutralization cannot be attributed to a change in the former. Pathways calculations indicate that the neutralization does not change either the area of reactive surface on Mb or the reactivity of that surface. Moreover, the additional intervening bonds introduced by methylation would, if anything, be expected to weaken the electronic coupling in a reactive configuration, rather than enhancing it. The argument that changing the propionates does not majorly change k_{et} is supported by the observation that the experimental values of k_2 for ZnMb(dme) and ZnMb(diamide) differ by less than a factor of 2, whereas charge neutralization, as represented by both, changes k_2 by over 2 orders of magnitude.

The increase can also not be associated with the nuclear term. This depends on the driving force of the ET reaction ($-\Delta G°$) and reorganization energy (λ). For the photoinitiated ET reaction of eq 1a, one can estimate $-\Delta G° \approx \lambda \approx 1$ eV.[37−39] Neutralization of the propionates would not influence λ significantly, while the change in the driving force upon heme neutralization is

(31) Measurements on the complex between cytochrome *c* peroxidase and cytochrome *c* suggest that these values will be less than those at lower protein concentrations.
(32) Leesch, V. W.; Bujons, J.; Mauk, A. G.; Hoffman, B. M. *Biochemistry* **2000**, *39*, 10132−10139.
(33) Frauenfelder, H.; Sligar, S. G.; Wolynes, P. G. *Science* **1991**, *254*, 1598−1603.
(34) Steinfeld, J. I.; Francisco, J. S.; Hase, W. L. *Chemical Kinetics and Dynamics*; Prentice-Hall: Englewood Cliffs, New Jersey, 1989.
(35) Liang, Z.-X.; Kurnikov, I. V.; Nocek, J. M.; Mauk, A. G.; Beratan, D. N.; Hoffman, B. M. **2002**, in preparation.
(36) Marcus, R. A.; Sutin, N. *Biochim. Biophys. Acta* **1985**, *811*, 265−322.

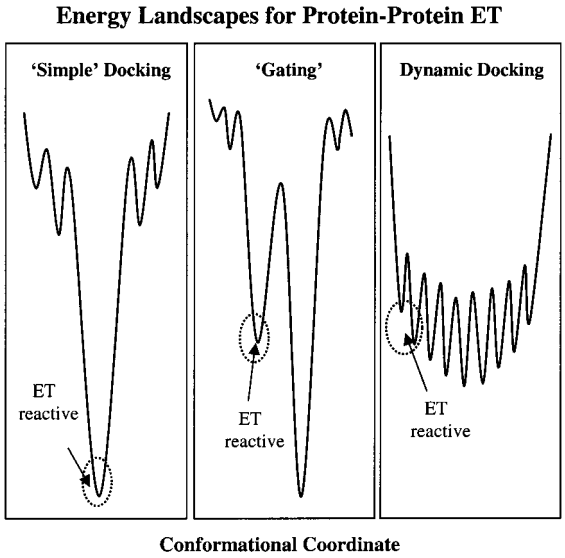

Figure 11. Schematic energy landscapes, which plot the conformational energy as a function of a "conformational coordinate" that connects the bound configurations of the complex,[33] for "simple docking", gated (or conformationally coupled) docking which involves two major conformational substrates, and dynamic docking, which involves multiple conformations of the complex.

expected to be no more than about 50 mV,[37] which is far too little to influence k_{et} substantially. In short, neutralization does not increase k_2 through changes in either K_a or k_{et}, *as defined within this simple model*. Thus, a more complex model is needed to understand the interaction and ET between ZnMb and cyt b_5.

Dynamic Docking (DD) Model. We now develop in detail a "dynamic docking" paradigm to describe ET reactions in weakly bound protein−protein complexes.[14] The model is shown to be supported by the experimental and computational results reported here, and in particular explains the consequences of heme neutralization.

The DD Model. This model postulates that cyt b_5 binds to Mb in a large ensemble of conformations at each of multiple sites on the Mb surface, each conformation being associated with its own rate constant for ET; the associated energy landscape is sketched in Figure 11. The binding picture is supported by the BD calculations (Figure 9, top), which show that cyt b_5 in fact docks onto a broad surface of native Mb that encompasses essentially the whole hemisphere incorporating the heme edge. Such a picture is likely to describe the binding of all systems, not merely Mb/cyt b_5 and Hb/cyt b_5[9,10,40] where affinities are low and there exist multiple conformations of the complex with comparable binding energy. Indeed, aspects of this model have been used in describing studies of ET within other complexes such as cytochrome *c*/cytochrome b_5, and cytochrome *c*/cytchrome *c* peroxidase.[22,25,41−43]

That each conformation must be assigned its own ET rate constant is required by the pathways ET coupling map, Figure 8, which in fact shows that only a small fraction of the Mb surface area near the heme edge is ET-active; this is incorporated in the DD energy landscape of Figure 11. Further, only a small fraction of those conformations with cyt b_5 bound at the reactive area actually will be reactive. Only conformations where the heme propionates of the two protein partners are in proximity ("edge-to-edge" conformation) would have high ET rate constants,[22] but the negative charges of the propionates also repel the partner proteins, thus suppressing these most reactive conformations. Instead, the repulsions would enhance the possibility that the unreactive "backside" of cyt b_5, and not the reactive front, would contact the reactive Mb surface.

The dynamic docking model, as formulated for ZnMb and cyt b_5, is described by the kinetic equations of eq 2. They describe two partners that bind in multiple interconverting conformations ($1 \rightarrow j$).

$$Zn^{*}Mb + (Fe^{3+})b_5 \left\{ \begin{array}{lll} \overset{K_a'}{\rightleftharpoons} & \{^{*}ZnMb/b_5\}_1 & \xrightarrow{k_{et}^{\,1}} \{^{+}ZnMb/(Fe^{2+})b_5\}_1 \\ \bullet\bullet\bullet & & \\ \overset{K_a^{\,i}}{\rightleftharpoons} & \{^{*}ZnMb/b_5\}_i & \xrightarrow{k_{et}^{\,i}} \{^{+}ZnMb/(Fe^{2+})b_5\}_i \\ \bullet\bullet\bullet & & \\ \overset{K_a^{\,j}}{\rightleftharpoons} & \{^{*}ZnMb/b_5\}_j & \xrightarrow{k_{et}^{\,j}} \{^{+}ZnMb/(Fe^{2+})b_5\}_j \end{array} \right. \quad (2)$$

Each conformation has its own ET rate constant, $k_{et}^{\,i}$, and its own microscopic binding free energy (ΔG_i) and binding constant, $K_a^{\,i} = \exp[-\Delta G_i/kT]$ (which can be expressed in terms of on- and off-rates, $k_{on}^{\,i}$, $k_{off}^{\,i}$, where $K_a^{\,i} = k_{on}^{\,i}/k_{off}^{\,i}$). The thermodynamic binding constant, K_a, which is measurable in an ITC or NMR experiment (or in kinetic titrations at high enough concentrations), is the sum of the individual binding constant ($K_a^{\,i}$) for all binding conformations (eq 3), both those that are ET-active and those that are not; the contribution of each configuration to the thermodynamic binding constant is describable in terms of a binding probability, g_i:

$$K_a = \sum_i K_a^{\,i} \qquad g_i = \frac{K_a^{\,i}}{K_a} \quad (3)$$

Kinetics in the Fast-Exchange or "Reaction Limit". As with the SD model, when the concentrations of the two reacting proteins are small as compared to the inverse of the binding constant, as in our ET measurements, the triplet-state ET quenching is characterized by a steady-state bimolecular ET rate constant, k_2. In this "thermodynamic", or "reaction", limit, we can ignore interconversion among bound complexes, and the steady-state formula for the DD second-order rate constant k_2 is a generalization of that for simple docking, $k_2 = \sum k_{et}^{\,i} \times k_{on}^{\,i}/(k_{off}^{\,i} + k_{et}^{\,i})$; this reduces to the SD formula when there is a single binding conformation, as required. In the fast-exchange reaction limit (see above), k_2 is the sum of the ET rate constants for all individual conformations, $k_{et}^{\,i}$, each weighted by the binding constant for that conformation (eq 4):

$$k_2 = \sum_i k_{et}^{\,i} K_a^{\,i} \quad (4)$$

One can recast this equation for k_2 into the same form as eq 1b, by partitioning k_2 into the product of the thermodynamic

(37) Reid, L. S.; Mauk, M. R.; Mauk, A. G. *J. Am. Chem. Soc.* **1984**, *106*, 2182−2185.
(38) Cowan, J. A.; Gray, H. B. *Inorg. Chem.* **1989**, *28*, 2074−2078.
(39) Dick, L. A.; Malfant, I.; Kuila, D.; Nebolsky, S.; Nocek, J. M.; Hoffman, B. M.; Ratner, M. A. *J. Am. Chem. Soc.* **1998**, *120*, 11401−11407.
(40) (a) Kidd, R. D.; Baker, E. N.; Brittain, T. *J. Biol. Inorg. Chem.* **2002**, *7*, 23−30. (b) Furukawa, Y.; Matsuda, F.; Ishimori, K.; Morishima, I. *J. Am. Chem. Soc.* **2002**, *124*, 4008−4019.
(41) Kostic, N. M. *Met. Ions Biol. Syst.* **1991**, *27*, 129−182.
(42) (a) McLendon, G. *Struct. Bonding (Berlin)* **1991**, *75*, 159−174. (b) McLendon, G.; Hake, R. *Chem. Rev.* **1992**, *92*, 481−490.
(43) Bendall, D. S. *Protein Electron Transfer*; BIOS Scientific Publishers: Oxford, 1996.

binding constant, K_a (eq 3), and a thermodynamically *averaged* intracomplex ET rate constant, k_{et}^{DD}, for a dynamically docked complex with multiple binding conformations

$$k_2 = k_{et}^{DD} K_a \tag{5a}$$

where k_{et}^{DD} is the sum of the ET rate constants (k_{et}^{i}) for each docked conformation, in this case as weighted by its binding *probability* (weighting factor g_i).

$$k_{et}^{DD} = \sum g_i k_{et}^{i} \tag{5b}$$

The first-order rate constant for intracomplex ET, k_{et}^{DD}, would be observed directly as the quenching constant under "saturating" conditions, when the concentration of cyt b_5 is high, complex formation is complete, and each Mb has a bound cytochrome. Even when concentrations are low, as here, this quantity can be calculated from measured values of k_2 and K_a, through use of eq 5a.

As discussed above, the k_{et}^{i} for most conformations are negligible, and the minority of reactive conformations having large k_{et}^{i} will dominate the summations for the rate constants, eqs 4, 5. In contrast, and as we now discuss further, in part because there are relatively few of these reactive conformations and in part because they do not have the most favorable binding energies, the thermodynamic binding constant (eq 3) is dominated by the nonreactive majority of conformations.

Effects of Heme Neutralization. The ET coupling map of native Mb (Figure 8) is not significantly altered by heme neutralization (not shown), but the BD simulations, Figure 9, show that charge neutralization causes a dramatic redistribution in the cyt b_5 docking locations, increasing the probability that cyt b_5 will dock within the ET reactive surface of ZnMb(dme). This is illustrated by the contact frequency histograms (Figure 10), which show that charge neutralization sharply increases the probability that residues located near the heme pocket make contact with the incoming cyt b_5. We now show that a DD model in which only a small number of the many docking conformations are ET-active explains how charge neutralization can cause a large change in k_2 (and k_{et}^{DD}) *without* substantially changing the overall thermodynamic binding constant, K_a.

The demonstration is simplified by considering an idealization of the model. We treat the members of the small fraction of highly reactive conformations (n_R in number; large k_{et}^{i}) as all having the same large ET rate constant, k_{et}^{R}, and the same binding constant, K_a^{R}. Likewise, we treat the large majority of nonreactive sites (N_{NR} in number) as having equal, but zero, reactivities, $k_{et}^{NR} = 0$, and equal (and most likely larger) binding constants, K_a^{NR}. As a result, eqs 3, 4 become

$$K_a = N_{NR} K_a^{R} + n_R K_a^{R} \tag{6a}$$

$$k_2 = k_{et}^{R} n_R K_a^{R} \tag{6b}$$

The first term of eq 6a corresponds to the affinity constant for the NR sites, the second to the affinity constant for the R sites.

Our experiments, BD, and pathways calculations indicate that for native Mb the nonreactive (NR) conformations dominate the binding, which translates into the inequality, $n_R K_a^{R} \ll N_R K_a^{NR}$; from this eq 6a gives $K_a \approx N_{NR} K_a^{NR}$. To a first approximation, charge neutralization should change *only* the energetics of binding in the reactive (R) conformations, increasing K_a^{R} but not k_{et}^{R}. This would change k_2 proportionally to K_a^{R} (eq 6b), while causing little-to-no change in K_a (eq 6a) as long as $n_R K_a^{R}$ remains less than $N_{NR} K_a^{NR}$. This *decoupling of binding from reactivity* is illustrated in Figure 12, which plots both the total affinity, K_a (eq 6a), and the reactivity, presented as k_2/k_{et}^{R} (eq 6b), as a function of the affinity of the R conformations, K_a^{R}, while the affinity of the NR conformations remains constant. Following the experimental results, the plot has taken the overall binding constant of native Mb for cyt b_5 to be $K_a \approx N_{NR} K_a^{NR} = 10^3\ M^{-1}$.

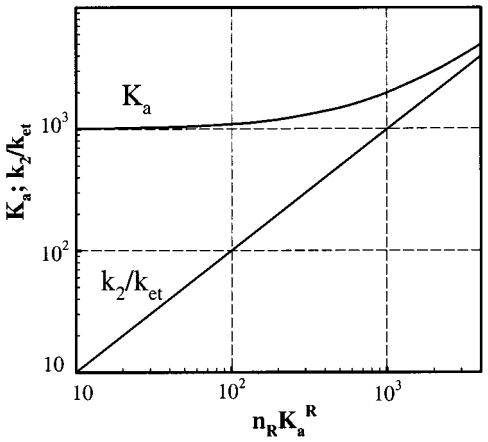

Figure 12. Plot of the predicted thermodynamic binding constant (K_a) and reactivity (k_2/k_{et}^{R}) versus the binding affinity for the reactive conformations ($n^{R}K_a^{R}$), according to eq 6, under the assumption that the affinity for the nonreactive conformations remains constant at ($N^{NR}K_a^{NR}$) = 1000 M^{-1}.

One sees that k_2 increases in proportion to K_a^{R}, while K_a indeed changes minimally so long as $n_R K_a^{R} \lesssim N_{NR} K_a^{NR}$. Consider the situation if the minority "reactive" conformations of the complex of cyt b_5 and native Mb contribute ~1% to the binding ($n_R K_a^{R}/N_{NR} K_a^{NR} = 10^{-2}$). If charge-neutralization increases K_a^{R} to the point that $n_R K_a^{R} \approx N_{NR} K_a^{NR}$, which equalizes the contribution of the R and NR sites to K_a, this would increase k_2 by 100-fold relative to the value in the native complex, but would increase K_a by a mere 2-fold (Figure 12). In fact, this heuristic calculation is consonant with the BD simulations in that the neutralization caused a very modest increase in the total number of hits (25 Å cutoff criterion), while it caused over a 100-fold increase in hits in the reactive region (~10 Å criterion).

It is useful to note the similarities and differences of this model to others which describe ET in a system with more than one conformation. As indicated in Figure 11, the well-known "gating" picture[44,45] involves a favored, nonreactive form of the complex plus a disfavored, but reactive form. A gated reaction occurs when the rate-limiting step is not the ET event, but rather it is the conformational switch. An alternate kinetic limit associated with the "gating" energy landscape is denoted "conformationally coupled" ET;[46] it involves a preequilibrium with the disfavored form, while the ET step remains rate limiting.

(44) Hoffman, B. M.; Ratner, M. R. *J. Am. Chem. Soc.* **1987**, *109*, 6237−6243.
(45) Hoffman, B. M.; Ratner, M. A.; Wallin, S. A. In *Advances in Chemistry Series*; Johnson, M. K., King, R. B., Kurtz, D. M., Jr., Kutal, C., Norton, M. L., Scott, R. A., Eds.; American Chemical Society: Washington, DC, 1990; Vol. 226, pp 125−146.
(46) Davidson, V. L. *Acc. Chem. Res.* **2000**, *33*, 87−93.

The DD model invokes a more complex energy landscape, with multiple conformations. In the rapid-exchange, or "reaction", limit of the model discussed here, k_2 is proportional to the actual ET rate constant, eq 4, in analogy to conformationally coupled ET. However, with the numerous dynamic docking configurations, the conformational influence in the DD model can be thought to occur in "phase space"; the observed rate is controlled by the relative accessibility of the few reactive configurations (Figure 11). However, just as the "gating" energy landscape can lead to "gating" or "conformational coupling", depending on relative rates of ET and conformational conversion, so too can the DD landscape exhibit an opposite, "gating-like" diffusion limit, as well as intermediate cases, where some conformations are in rapid exchange, others not, and cases where interconversion among bound conformations (conformational coupling) is kinetically important.

BD Calculations and Ionic Strength/pH Effects. The experimentally determined ionic strength dependence of k_2 for ZnMb(dme) is far stronger than that for ZnMb, Figure 4. Such behavior is observed in the BD docking profiles for ZnMb and ZnMb(dme); both show broad docking regions at high ionic strength (200 mM), whereas they are sharply different at 18 mM ionic strength (Figure 9). This confirms that the enhanced reactivity produced at low ionic strength by charge neutralization comes from favorable electrostatic effects, and shows that these are screened at high ionic strength, in effect nullifying the benefits of charge neutralization in increasing k_2 at low ionic strength.

The pH dependence of k_2 (Table 1) can be partitioned into the joint pH dependence of the overall binding affinity K_a, and of the reactivity, k_{et}^{DD}, which depends on binding specificity, eq 5. A change of K_a with pH is suggested by the ITC measurements. A change of binding specificity with pH is indicated by the BD simulations. For example, for ZnMb, more complexes are formed at pH 6.0 than at pH 8.0, consistent with an increase in K_a, but more importantly, many more complexes with shorter donor−acceptor distance (i.e., reactive complexes) are formed at pH 6.0.[8] In contrast, for ZnMb(dme), simulations show that pH change has a modest effect on both the total number of complexes and the enhanced proportion of reactive complexes (data not shown). These simulation results are consistent with the experimental result that a change from pH 6.0 to pH 8.0 causes a large decrease (∼30-fold) in k_2 for ZnMb and a small decrease (∼3-fold) in the much larger k_2 for ZnMb-(dme).

Conclusions

The neutralization of the two heme propionates of ZnMb by formation of the heme diester, or for the first time the diamide, increases the second-order rate constant of the ET reaction between ZnMb and cyt b_5 by as much as several 100-fold, depending on pH and ionic strength, while causing a negligible enhancement in binding affinity. These results, in conjunction with pathways calculation and BD simulations, lead to a dynamic docking model for complex formation and ET reactivity in which reaction rates are effectively decoupled from binding affinities. Analogous results for the reaction of cyt b_5 with Hb show that the DD model applies there, too.[9,10]

The DD model, whose energy landscape[33] is indicated in Figure 11, pictures the Mb/Hb surface as a large "target" with a small "bullseye" for the cyt b_5 "arrow". The model asserts that cyt b_5 binds to a large area on the Mb/Hb surface, in a wide variety of docked conformations, but that ET involves only a small subset of highly ET-reactive conformations in which cyt b_5 is bound near the Mb/Hb heme edge and that this subset does not involve the most stable binding configurations. The probability of binding in the reactive Mb/Hb surface region is low, in part because repulsive electrostatic interactions between the negatively charged propionates of Mb/Hb and cyt b_5 act to suppress the highly ET reactive conformations. Neutralization of the Mb/Hb propionates eliminates these repulsive interactions and increases the probability of achieving a reactive conformation, but without appreciably influencing the overall binding, which is dominated by the more numerous nonreactive conformations. This decoupling of reactivity and binding does not, in fact, depend on details of the kinetic model discussed here, but only on the existence of a DD energy landscape such as that depicted in Figure 11.

These results support the idea that in these complexes, and possibly others, electrostatic interactions can play an important role in directing "productive" protein docking without contributing to the overall binding energy.[41,47] The resulting decoupling of reactivity from binding affinities is physiologically important in the cases of Mb and Hb, where high affinities would hinder efficient interprotein ET; the same may be true for other protein−protein interactions.

Acknowledgment. The work has been supported by the National Institutes of Health (HL62303 [B.M.H.] and GM48043 [D.N.B.]) and by the Division of Chemical Sciences, Office of Science, U.S. Department of Energy (DE-FG02-99-ER14999 [R.T.H.[48]]). We would like to thank Mr. Steven Lowe and Professor Katharyn Thomasson for help with the BD simulations. We acknowledge the use of the ITC calorimeter in the Keck Biophysics Facility at Northwestern University.

JA0127032

(47) Camacho, C. J.; Vajda, S. *Proc. Natl. Acad. Sci. U.S.A.* **2001**, *98*, 10636−10641.
(48) Grant to Prof. M. Wasielewski.